

Fast measurements of entanglement over a kilometric distance to test superluminal models of Quantum Mechanics: final results.

B Coccia¹, S Faetti² and L Fronzoni²

¹ High School XXV Aprile, Via Milano 2, I-56025 Pontedera (Pisa), Italy

² Department of Physics Enrico Fermi, Largo Pontecorvo 3, I-56127 Pisa, Italy

E-mail: b.coccia@comeg.it, sandro.faetti@unipi.it, leone.fronzoni@unipi.it

Abstract. Quantum mechanics is a non local theory. To recover the locality principle some physicists suggested that the correlations between entangled particles could be established by communications propagating with a velocity $v_t > c$ in a preferred frame. In the previous DICE conference we reported the preliminary results of a high sensitivity experiment to test the superluminal models. Here we report the final results. No breaking of the quantum predictions has been found. Then, we infer that the velocity of the quantum communications has to be higher than a lower bound of the order of some millions of times the light velocity.

1. Introduction

1.1. The non-locality of quantum mechanics and the superluminal models.

In 1935 Einstein, Podolsky and Rosen (EPR-paradox) [1] showed that orthodox quantum mechanics is a non-local theory. Consider photons a and b in Figure 1 that are in the maximally entangled state

$$|\psi\rangle = \frac{1}{\sqrt{2}} (|H, H\rangle + |V, V\rangle), \quad (1)$$

where H and V denote horizontal and vertical polarization, respectively. Photons a and b impinge on two absorption polarizers P_A and P_B with the polarization axes that make the angles α and ξ with respect to the horizontal axis. Quantum mechanics predicts that the probability that photon a (or b) passes through a polarizer is $p = 1/2$ for any polarizer orientation. Furthermore, if one photon passes first through polarizer P_A having the polarization axis at angle α and is detected by the photon counter, the entangled state in eq.(1) collapses *instantaneously* to the state $|\alpha_a, \alpha_b\rangle = |\alpha_a\rangle |\alpha_b\rangle$ where $|\alpha_a\rangle$ and $|\alpha_b\rangle$ denote single photon states linearly polarized at the same angle α . This means that the polarization measurement at point A affects instantaneously the result of the polarization measurement at point B (*spooky action at a distance*). The probability that both photons pass through the polarizers is $P(\alpha, \xi) = \frac{1}{2} \cos^2(\alpha - \xi)$. Einstein, Podolsky and Rosen[1] concluded that quantum mechanics is an incomplete theory and suggested that a complete local theory should contain some additive local variables (“hidden variables” in the literature). Before 1964, the choice between orthodox quantum mechanics and local variables models was just a matter of personal taste but, in 1964, J. Bell [2] demonstrated that any theory



Content from this work may be used under the terms of the [Creative Commons Attribution 3.0 licence](#). Any further distribution of this work must maintain attribution to the author(s) and the title of the work, journal citation and DOI.

based on local variables must satisfy an inequality that is violated by Quantum Mechanics. Analogous inequalities have been proposed by Clauser et al. [3, 4](the Bell-Clauser-Horne-Shimony-Holt inequality). Then, a direct experimental comparison between quantum mechanics and local variables models became possible.

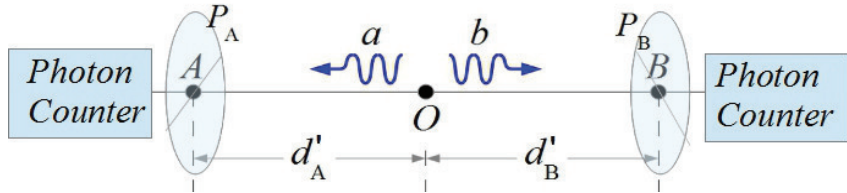


Figure 1. Two entangled photons a and b are generated at O , get the absorption polarizing films P_A (Alice polarize) and P_B (Bob polarizer) and are collected by photon counting modules.

In 1982 Aspect et al. [5] found that the Bell inequality is violated and also showed that the quantum correlations at a distance cannot be induced by luminal communications. Other successive experiments confirmed the Aspect et al. results and also closed some residual loopholes [6, 7, 8, 9]. Despite the remarkable successes of orthodox quantum mechanics, some physicists are very reluctant to abandon the principle of locality and are still looking for alternative local theories. Newton himself in a letter to R. Bentley [10] expressed a strong criticism on action at distance and wrote

“That gravity should be innate, inherent, and essential to matter, so that one body may act upon another at a distance through a vacuum, without the mediation of anything else, by and through which their action and force may be conveyed from one to another, is to me so great an absurdity that I believe no man who has in philosophical matters a competent faculty of thinking can ever fall into it.”

The Newton reluctance to accept the idea of a nonlocal behavior of the Nature found a strong support in the successive history of Physics. In fact, at the beginning of the 20th century Einstein showed that the gravitational interactions are not instantaneous but are established by exchange of gravitational waves that have been recently detected[11]. A similar behavior characterized the history of the electric interactions. For this reason, some physicists think that suitable communications could explain the apparent nonlocality of the quantum correlations. After that the Aspect et al. experiment [5] showed that these eventual communications cannot travel with luminal or subluminal velocities, J. Bell, in a famous interview, said: “ *in these EPR experiments there is the suggestion that behind the scenes something is going faster than light*” (see page 49 in [12]). To avoid causal paradoxes, the superluminal communications must propagate in a preferred frame at a velocity $v_t = \beta_t c$ higher than the light speed where $\beta_t = v_t/c$ is the adimensional velocity. The existence of a preferred frame is needed to avoid causal paradoxes but Refs. [13, 14] strongly stressed that it is not in contrast with the relativity theory. Note that a preferred frame has been already observed: it is the Cosmic Microwave Background frame (CMB frame) that moves with the adimensional velocity $\beta \approx 10^{-3}$ with respect to the Earth geocentric frame. Of course, the CMB frame could be a good candidate as a preferred frame for the superluminal communications. Eberhard[15] and Bohm and Hiley[16] developed specific superluminal models based on this idea (v -causal models in the current literature [17]). Superluminal communications between only two entangled particles could not be used to exchange information in the macroscopic world (*signalling*), but it was recently shown[18, 19] that superluminal communications between three or four entangled particles allow signalling. Although one of us believes that signalling is not in a strict conflict with the relativity theory [13, 14], most physicists think that there is complete incompatibility between signalling and

relativity. According to them, the experimental evidence of signalling would need a revision of the relativity theory. Anyway, we stress here the Physics is an experimental matter and only the experiment can give a definitive answer.

1.2 The method to test the superluminal models.

It is important to emphasize that in our experiment we use absorption polarizers and not polarizing beamsplitters. When a photon impinges on an absorption polarizer, it is either absorbed or transmitted by the polarizer and, thus, we think that the outgoing state is not a pure quantum state but is a quantum mixture of a vacuum state (absorbed photon) and a linearly polarized state (transmitted photon). If a successive detection of the photon occurs, one can infer that the photon has not previously absorbed and that it was already linearly polarized just at the exit of the polarizer. Then, we make here the assumption that the collapse of the polarization state of the photon occurs at the absorption polarizer and not at the detector. Here we consider all the possible superluminal models, as well as the Eberhard one, where a first event (the passage of a photon through a polarizer) affects a second event (the passage of the other photon through the second polarizer) via a superluminal communication. If photon a goes first (in the preferred frame) through polarizer P_A , it does not induce the instantaneous collapse of the entangled state to the state $|\alpha_a\rangle|\alpha_b\rangle$ but only the local collapse of the state of photon a to $|\alpha_a\rangle$. The collapse of the second photon to the linear polarized state $|\alpha_b\rangle$ will occur only when a collapsing superluminal wave reaches it. The collapsing wave propagates isotropically in the preferred frame at the adimensional superluminal velocity β_t ($\beta_t > 1$) and is created where (and when) the first event occurs (e.g. a photon hits a polarizer). The first event is the one which occurs temporally before in the preferred frame. For $\beta_t \rightarrow \infty$, the collapse occurs instantaneously everywhere and the superluminal model leads to the same predictions of quantum mechanics. If polarizers P_A and P_B are at the same distances d'_A and d'_B from the source O of the entangled photons in the preferred frame, the two photons get to the polarizers simultaneously (the wavepackets width is disregarded here) and no communication is possible if β_t has a finite value. Then, probability $P(\alpha, \xi)$ must satisfy the local Bell-Clauser-Horne-Shimony-Holt inequality and the correlation parameter

$$S_{max} = P_0 - \sum_{i=1}^3 P_i, \quad (2)$$

with $P_0 = P(45^\circ, 67.5^\circ)$, $P_1 = P(0^\circ, 67.5^\circ)$, $P_2 = P(45^\circ, 112.5^\circ)$ and $P_3 = P(90^\circ, 22.5^\circ)$ must satisfy the inequality $S_{max} \leq 0$ [20, 21] while quantum mechanics predicts $S_{max} = (\sqrt{2}-1)/2 \approx 0.2071$. Probabilities $P(\alpha, \xi)$ can be experimentally obtained using the relation

$$P(\alpha, \xi) = \frac{N(\alpha, \xi)}{N_{tot}}, \quad (3)$$

where $N(\alpha, \xi)$ are the coincidences between entangled photons passing through the polarizers during the acquisition time δ_{at} and N_{tot} is the total number of entangled photons couples that can be also written in the form:

$$N_{tot} = \sum_{i=0}^3 N_i, \quad (4)$$

where $N_0 = N(0^\circ, 0^\circ)$, $N_1 = N(0^\circ, 90^\circ)$, $N_2 = N(90^\circ, 0^\circ)$ and $N_3 = N(90^\circ, 90^\circ)$. Due to the experimental uncertainty, the arrival times of the photons at the polarizers could differ by a quantity $\Delta t' = \Delta d'/c$ where $\Delta d'$ is the uncertainty of the *effective optical paths difference* that takes into account the uncertainty of the optical path difference but also any other source of

spatial uncertainty [for a detailed analysis of the error sources see Eq.(7) in [21]]. In such a case, a superluminal communication would be impossible only if $\Delta t'$ is smaller than the time $\Delta t'' = d'_{AB}/(\beta_t c)$ that is needed to establish a communication between points A and B , where d'_{AB} is the optical path from A to B in the preferred frame (see Figure 1). The condition $\Delta t' < \Delta t''$ is satisfied if β_t is lower than a maximum detectable value $\beta_{t,max} = d'_{AB}/\Delta t'$. Therefore, a breakdown of the quantum predictions ($S_{max} < 0$) could be observed in the preferred frame only if $\beta_t < \beta_{t,max}$.

On the Earth laboratory frame the analysis is more complex. The time difference $\Delta t'$ in the preferred frame is related to that in the laboratory frame by the Lorentz relation:

$$\Delta t' = \gamma(\Delta t - \vec{\beta} \cdot \vec{AB}), \quad (5)$$

where $\vec{\beta}$ is the unknown adimensional relative velocity vector of the preferred frame with respect to the laboratory frame and \vec{AB} is the vector that connects points A and B in the laboratory frame. The detection of the superluminal effects requires that $\Delta t'$ is as small as possible to satisfy the condition $\Delta t' < \Delta t''$. However a small value of the time uncertainty in the laboratory frame ($\Delta t \approx 0$) does not imply $\Delta t' \approx 0$ except if $\vec{\beta} \cdot \vec{AB} \approx 0$ in Eq.(5). If the AB segment is east-west aligned, due to the earth's rotation around its axis, there are always two times t_1 and t_2 for each sidereal day where \vec{AB} becomes orthogonal to $\vec{\beta}$ [22, 23]. Our experiment is performed inside the so called east-west gallery of the European Gravitational Observatory (EGO)[24] that is not aligned along the east-west axis but makes the angle $\gamma = 18^\circ = \pi/10$ with it. In this case, the condition $\vec{\beta} \cdot \vec{AB} = 0$ is still verified at two times t_1 and t_2 each sidereal day except if the velocity vector of the preferred frame makes a polar angle $\chi < |\gamma| = \pi/10$ or $\chi > \pi - |\gamma| = 9\pi/10$ with respect to the Earth rotation axis (see Figure (2)). This means that our experiment is virtually insensitive to the fraction $\Omega/(4\pi) = \int_0^\gamma \sin \theta d\theta < 5\%$ of all the possible alignments of the preferred frame velocity vector. Note that the reference frame of the Cosmic Microwave Background ($\chi \approx 97^\circ$) is accessible to our experiment.

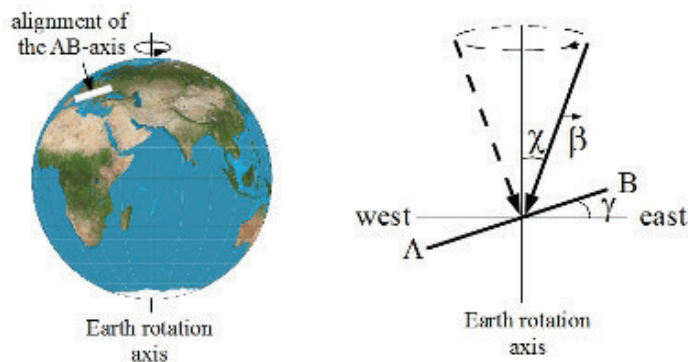


Figure 2. The velocity vector $\vec{\beta}$ with respect to the laboratory frame rotates on a cone of angle χ around the Earth axis (the small contributions due to the rotation of the Earth around the Sun and to the precession and nutation of the Earth axis are disregarded here). The angle between vector $\vec{\beta}$ and segment AB varies between $\pi/2 - \gamma - \chi$ and $\pi/2 - \gamma + \chi$. Then, $\vec{\beta}$ become orthogonal to AB only if $\pi - |\gamma| \geq \chi \geq |\gamma|$.

For $\pi - |\gamma| \geq \chi \geq |\gamma|$, the maximum measurable superluminal velocity is[22] (see also Eqs.(6) and (7) in Ref.[25]):

$$\beta_{t,max} = \sqrt{1 + \frac{(1 - \beta^2)[1 - \rho^2]}{\left[\rho + A \frac{2\pi\beta\delta_a t}{T}\right]^2}}, \quad (6)$$

where

$$A = \sqrt{\sin^2 \chi \cos^2 \gamma - \cos^2 \chi \sin^2 \gamma}. \quad (7)$$

T is the earth rotation day and $\rho = d_{AB}/\Delta d$, where d_{AB} is the optical path between points A and B in the laboratory frame. Parameter $\beta_{t,max}$ greatly decreases out of the interval $\pi - |\gamma| \geq \chi \geq |\gamma|$ [22]. If $\beta_t < \beta_{t,max}$, each day close to times t_1 and t_2 the parameter S_{max} should jump from the quantum value $S_{max} = 0.2071$ to the Bell-Clauser-Horne-Shimony-Holt value $S_{max} \leq 0$.

Some experimental tests of the superluminal models have been performed but no violation of the quantum mechanics predictions has been found and only lower bounds $\beta_{t,max}$ for the velocity β_t of the superluminal signals have been established [22, 23, 26, 21]. In the previous Conference we reported some preliminary results of an improved experiment and here we report the final results [25] where the maximum detectable velocity of the superluminal communications is increased by about two orders of magnitude.

2. Experiment.

2.1. The experimental apparatus and procedures.

To increase the value of the maximum detectable adimensional velocity $\beta_{t,max}$, one has to make the experimental parameters ρ and $\delta_a t$ in Eq.(6) as small as possible. To get a small value of $\rho = d_{AB}/\Delta d$ we exploit the large distances available in the EGO gallery ($d_{AB} \approx 1200$ m) and we use an interferometric method to equalize the optical paths d_A and d_B within $5 \mu\text{m}$ ($d_A \approx d_B \approx 600$ m). The final uncertainty $\Delta d \approx 0.22$ mm of the equality of the effective optical paths is due to many error sources including (in order of relevance) the finite thickness of the polarizing layers, the air dispersion, the uncertainty of the interferometric measurement, and the wavepackets width (the analysis of the error sources is given in [21]). To get a very small acquisition time $\delta_a t$ we develop a high intensity source of entangled photons and we minimize photons losses using a suitable optical apparatus and feedback procedures to stabilize the photons paths.

The experimental apparatus has been already described in detail in Ref. [21] and, thus, we show only a very simplified scheme in Figure 3 where the four reference optical beams used to stabilize the propagation of the entangled photons beams and to equalize the optical paths are not shown. Figure 3 a) shows the system used to generate a high intensity beam of entangled photons with a sufficient purity (Fidelity > 0.95). A pump laser beam is polarized at 45° with respect to the horizontal axis by a polarizer, passes through a $\lambda/2$ plate, a Babinet-Soleil compensator, a compensating plate C and is focused (spot diameter equal to 0.6 mm) at the center of two adjacent BBO nonlinear optical crystal plates (29.05° tilt angle, 0.56 mm-thickness) cut for type I phase matching [27]. The BBO plates have the optical axes lying in the horizontal and vertical plane, respectively. Down-conversion generates two outgoing beams of entangled photons at the average wavelength $\lambda = 2\lambda_p = 812.6$ nm that mainly propagate at two symmetric angles ($\pm 2.42^\circ$) with respect to the normal to the crossed BBO plates. The entangled beams are deviated in opposite directions along the EGO gallery by two right-angle prisms, pass through the diaphragmed compensating plates C_A and C_B and exit from the central table. Plates C , C_A and C_B are used to increase the purity of the entangled state [28, 29, 30]. In such a way we get a high-intensity source of entangled photons ($N_{tot} \approx 23000$ coincidences/s) in an entangled state of sufficient purity. The beams outgoing from the central table are collected by two large achromatic lenses L_A and L_B having a 6 m focal length and a 15 cm diameter as shown in Figure 3 b). The

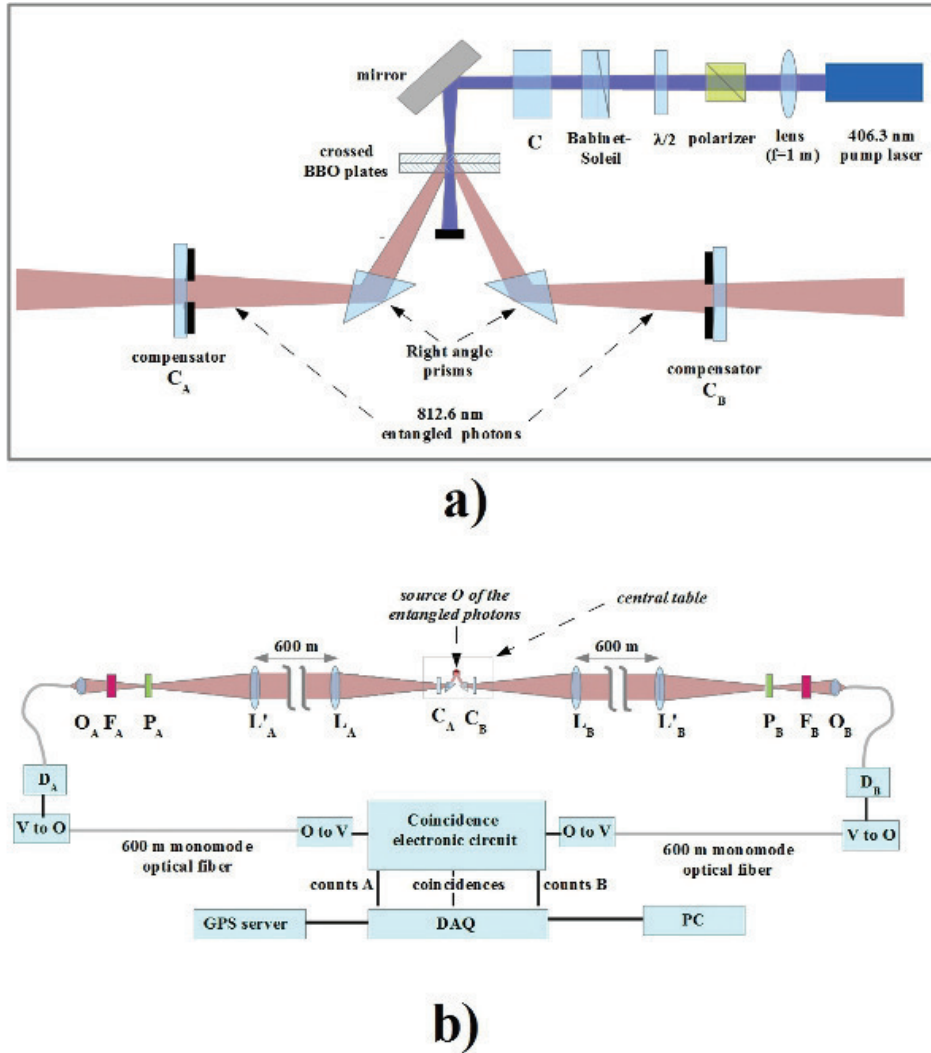


Figure 3. a) The optical apparatus to generate high intensity beams of entangled photons. C , C_A and C_B are anisotropic compensator plates used to get a sufficient fidelity of the entangled state. The pump beam is focused at the centre of two crossed adjacent BBO plates (29.05° tilt angle) where entangled photons are generated and emitted at the average angles $\pm 2.42^\circ$ with respect to the pump laser beam. The whole system is thermostated within 0.1°C . b) The optical scheme used to produce a 1:1 real image of the source O of the entangled photons on polarizers P_A and P_B at about 600 m from O . The figure is not to scale. L_A , L_B , L'_A and L'_B are specially designed 15 cm-diameter achromatic lenses aligned along the EGO gallery and having a 6.00 m. P_A and P_B are absorption polarizing filters. F_A and F_B are sets of adjacent optical filters, O_A , O_B are optical lenses, D_A and D_B are photon counting detectors. V to O are electronic systems that transform the output voltage pulses into optical pulses, whilst O to V transform the optical pulses into voltage pulses. DAQ is a National Instruments CompactDAC that provides a real time acquisition of coincidences.

transmitted beams propagate along the gallery and impinge on two identical achromatic lenses L'_A and L'_B at a distance approximately 600 m from the source O in the figure. Two real 1:1 images (0.6 mm wide) of the source of the entangled photons are produced at the centers of the linear absorption polarizers P_A and P_B (Thorlab LPNIR). Four reference beams at wavelength $\lambda_R = 681$ nm (not shown in the Figure but extensively described in Ref.[21]) are utilized to align the optical system, to equalize the optical paths and to keep under control the deviations of the entangled beams due to the air turbulence and to the vertical gradients of the air refractive index. In this way the spots of the entangled beams on the polarizers remained fixed within ± 0.4 mm during the whole 8 days measurement time. Each of the entangled photons beams outgoing from the two polarizers P_A or P_B passes through a filtering set (F_A or F_B in Figure 3 b)) made by two long-pass optical filters ($\lambda_c = 765$ nm) that stop the reference 681-nm beams and a bandpass filter ($\lambda = 810$ nm ± 20 nm). Then, each beam is focused by a system of optical lenses (O_A or O_B) on a multimode optical fiber having a large numerical aperture (0.39) and a core diameter of 200 μm connected to a Perkin Elmer photons-counter module. The output pulses of the photons counters are transformed into optical pulses (using the LCM155EW4932-64 modules of Nortel Networks) that propagate in two monomode optical fibers toward the central optical table where the entangled photons are generated. Finally, the optical pulses are transformed again into electric pulses and sent to an electronic coincidence circuit. An electronic counter connected to a National Instruments CompactDAQ counts the Alice pulses N_A , the Bob pulses N_B , and the coincidences pulses N .

2.2. The fast acquisition procedure

In the previous Conference DICE 2016[21] we reported some preliminary results where the measurements of the probabilities $P_i = P(\alpha_i, \xi_i)$ ($i = 0, 1, 2, 3$) appearing in eq.(2) were made sequentially. The procedure needed some consecutive rotations of the polarizers before a single value of S_{max} was obtained leading to a long acquisition time $\delta_{at} \approx 100$ s for each measurement of S_{max} . In the final experiment the acquisition time δ_{at} has been greatly reduced measuring each of the four probabilities P_i in successive daily experimental runs. The polarization angles α_i and ξ_i are set before the beginning of each i -th run made of 2^{19} successive acquisitions of the coincidences $N(\alpha_i, \xi_i)$ and the corresponding probabilities $P_i = N(\alpha_i, \xi_i)/N_{tot}$ are obtained. The procedure is fully automatized using a National Instruments CompactDAQ where a real time LABVIEW program runs. The real time procedure ensures a full continuity of the acquisitions and a constant acquisition time. The values of parameters ρ and δ_{at} are

$$\rho = 1.83 \times 10^{-7}, \delta_{at} = 0.247 \text{ s.} \quad (8)$$

A Global Positioning System (GPS) Network Time Server (TM2000A) provides the actual Coordinated Universal Time (UTC) [31, 32] with an absolute accuracy better than 1 ms. Since the investigated phenomenon is related to the Earth's rotation, we synchronize the acquisitions with the Earth's rotation time $t = \theta \times 240$ s where θ is the Earth Rotation Angle(ERA) [33] expressed in degrees. The synchronization procedure is fully automatized and it ensures that each acquisition run starts at the UTC time that corresponds to the zero Greenwich Earth rotation time[25]. Four acquisition runs each with a duration of 36 Earth rotation hours (about 35 h, 54 min, and 7 s in the standard UTC time) are performed to obtain the four probabilities P_i with $i = 0, 1, 2, 3$ that appear in Eq.(2). The spurious statistical coincidences are subtracted.

3. Results and conclusions.

Figures 4(a)-4(d) show the probabilities $P_i = P(\alpha_i, \xi_i) = N(\alpha_i, \xi_i)/N_{tot}$ obtained in the successive runs ($i = 0, 1, 2, 3$). Due to the large number of points (2^{19}) acquired in each run, the experimental measured values are distributed within a black region having a thickness of several standard

deviations. Note the great stability of our equipment that ensured the full continuity of the measurements without any interruption during the whole measuring time (about 8 days). The solid green line represents the average value, and the green dotted line represents the value predicted by quantum mechanics for the pure maximally entangled state in Eq.(1) (fidelity $F = 1$). The discrepancy between the solid and dotted lines indicates that either our entangled state is not completely pure ($F \approx 0.95$) or some systematic noise is present. The experimental results in Figures 4(a)-4(d) do not exhibit any evident peak outgoing from the noise region and, thus, no apparent breakdown of the quantum mechanics predictions. Assuming that the investigated phenomenon has the same periodicity as the Earth rotation, one can calculate the S_{max} value at each Earth rotation time by substituting into the theoretical expression of S_{max} in Eq.(2) the P_i contributions of Figure 4 measured at the same Earth rotation time t in the successive runs.

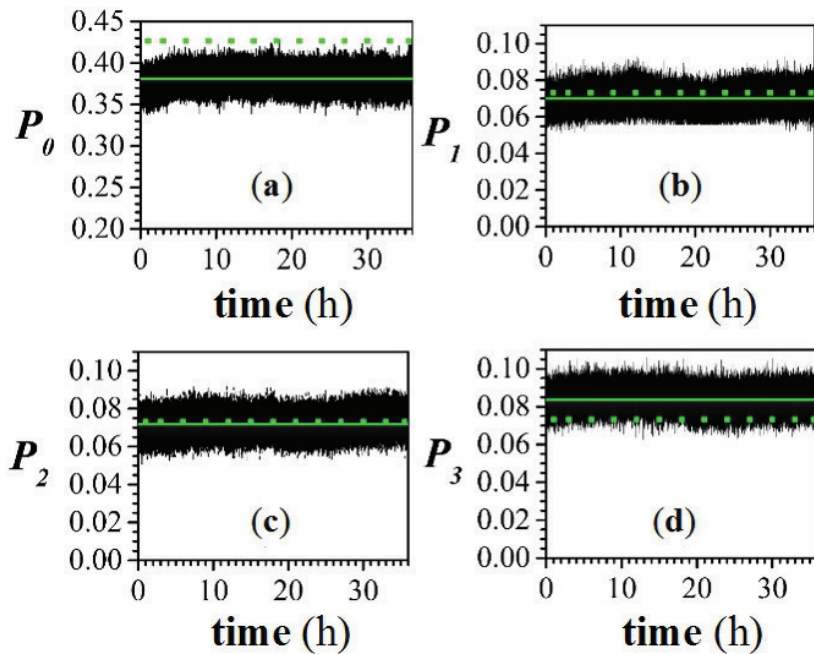


Figure 4. Probabilities **a)** P_0 , **b)** P_1 , **c)** P_2 and **d)** P_3 measured in successive runs versus the Greenwich earth rotation time. The 2^{19} values measured in each run are connected by straight lines leading to the resulting black regions in the figure. The acquisition time is $\delta_a t \approx 0.247$ s. The green solid lines represent the average values of the measured probabilities: $\langle P_0 \rangle \geq 0.38087$, $\langle P_1 \rangle \geq 0.06999$, $\langle P_2 \rangle \geq 0.07187$, $\langle P_3 \rangle \geq 0.08378$. The green dotted lines correspond to the values predicted by quantum mechanics for a pure maximally entangled state: $P_0 = 0.4267$, and $P_1 = P_2 = P_3 = 0.0732$.

With this procedure we get the results shown in Figure 5(a) (black region) and the corresponding frequency distribution ρ_0 shown in Figure 5(b) where black points represent the experimental results and the solid green line is the best fit with the Gaussian function $A \exp [-(S_{max} - \langle S_{max} \rangle)^2 / (2\sigma^2)]$ with standard deviation $\sigma = 0.01272$ and $\langle S_{max} \rangle = 0.15523$. The green solid line in Figure 5(a) shows the average value $\langle S_{max} \rangle$ and the green dotted line is the quantum mechanics value $S_{max} = 0.2071$ for the maximally entangled state in Eq.(1) ($F = 1$). Unfortunately, the phenomenon that is investigated here has not exactly the same periodicity

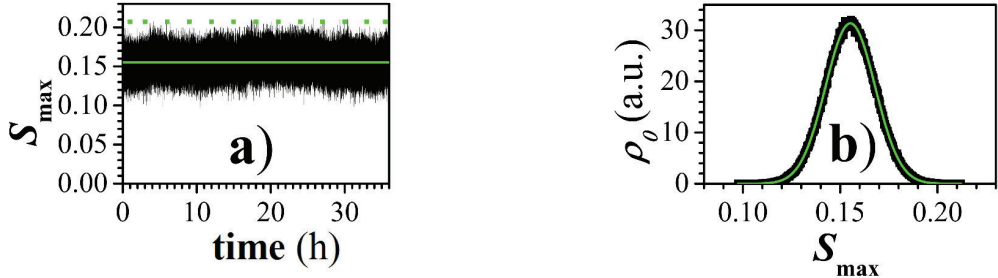


Figure 5. a) Parameter S_{max} versus the earth rotation time obtained using the relation $S_{max}(t) = P_0(t) - P_1(t) - P_2(t) - P_3(t)$. The green solid line is the average value $\langle S_{max} \rangle = 0.15523$, while the green dotted line represents the quantum mechanics average value $\langle S_{max} \rangle = 0.207$ predicted for the pure maximally entangled state in Eq.(1). b) Frequency distribution ρ_0 of the 2^{19} measured values of S_{max} in arbitrary units. The solid green curve is the Gaussian fit with standard deviation $\sigma = 0.01272$ and $\langle S_{max} \rangle = 0.15523$.

as the Earth rotation because the breaking of quantum mechanics should occur when vector $\vec{\beta}$ becomes orthogonal to vector \vec{AB} . Due to the revolution motion of the earth around the sun and other minor motions (precession and nutation of the Earth's axis), vector $\vec{\beta}$ does not return exactly to the same orientation with respect to the laboratory frame after one Earth rotation day. Denote by t_{i1} and t_{i2} the successive two unknown times during the i -th measurement run ($i = 0-3$) where the orthogonality condition $\vec{\beta} \cdot \vec{AB} = 0$ is satisfied and by $P_i(t_{ij})$, with $i = 0-3$ and $j = 1, 2$, the probabilities P_0 , P_1 , P_2 and P_3 measured at these times in the successive runs ($i = 0-3$). If $\beta_t < \beta_{t,max}$, all or some of these probabilities should be different from the quantum mechanics values and the correlation parameters

$$S_{max}(j) = P_0(t_{0j}) - \sum_{i=1}^3 P_i(t_{ij}) \quad (9)$$

should satisfy the Bell-Clauser-Horne-Shimony-Holt inequality.

We do not know what are the times t_{ij} and we cannot calculate $S_{max}(j)$ but it is obvious that $S_{max}(j) \geq S = MIN(P_0) - MAX(P_1) - MAX(P_2) - MAX(P_3)$ where $MIN(P_i)$ and $MAX(P_i)$ are the absolute minimum and maximum measured values of P_i during each acquisition run, respectively. From the experimental data in Figure 4 we get $S = 0.04237$ and thus $S_{max}(j) \geq 0.04237 \approx 3.3\sigma$. The probability that a value of $S_{max}(j)$ lower than or equal to zero could be compatible with our measured values is $p \leq \frac{1}{2}\text{erfc}\left[0.04237/(\sqrt{2}\sigma)\right] = 4.3 \cdot 10^{-4}$, where $\text{erfc}(x)$ is the complementary error function. At least two breakdowns of S_{max} should occur during the time of 36 h and the probability P that both these breakdowns happen here is $P = p^2 \sim 2 \times 10^{-7}$. Then, we can conclude that there is no evidence of a breakdown of the quantum mechanics predictions and that the velocity of the superluminal signals has to be higher than the maximum measurable value $\beta_{t,max}$.

Substituting $\rho = 1.83 \times 10^{-7}$ and $\delta_a t = 0.247$ s in Eq.(6) we obtain the lower bound $\beta_{t,max}$ of the superluminal velocities as a function of the unknown adimensional velocity β ($\beta < 1$) of the preferred frame and of the angle χ . According to Eq.(6), $\beta_{t,max}$ reaches the maximum value at the borders $\chi = |\gamma|$ and $\chi = \pi - |\gamma|$ of the region accessible to our experiment and the minimum value at $\chi = \pi/2$. Curve-a in Figure 6 shows our $\beta_{t,max}$ versus the unknown adimensional velocity β of the preferred frame in the unfavorable case $\chi = \pi/2$. In the case of the Cosmic

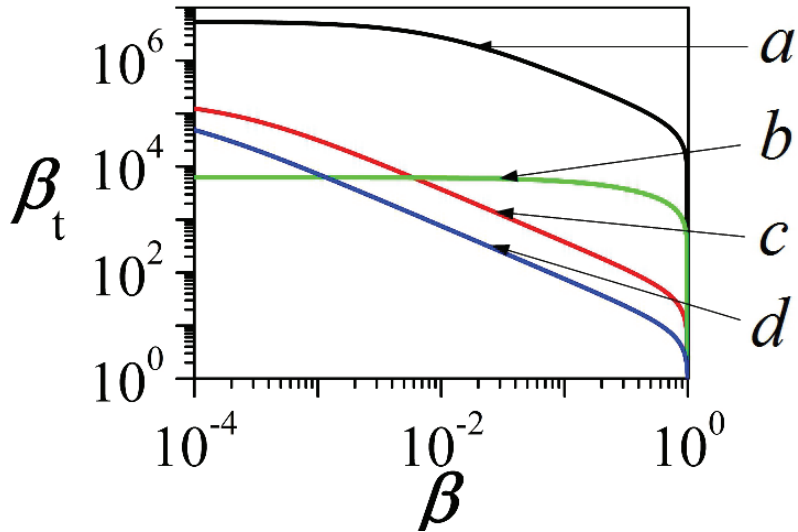


Figure 6. Curve *a* shows the $\beta_{t,\max}$ values obtained in our experiment using Eq.(6) ($\rho = 1.83 \times 10^{-7}$, $\delta_{at} = 0.247$ s, and $\gamma = 18^\circ$) versus the unknown adimensional velocity β of the preferred frame for $\chi = \pi/2$; curve *b* is the result obtained in Ref. [23] ($\rho = 1.6 \times 10^{-4}$, $\delta_{at} = 4$ s and $\gamma = 0^\circ$); curve *c* is the result obtained in Ref. [22] ($\rho = 5.4 \times 10^{-6}$, $\delta_{at} = 360$ s and $\gamma = 5.9^\circ$) and curve *d* is the result obtained in Ref. [26] ($\rho = 7.3 \times 10^{-6}$, $\delta_{at} = 1800$ s and $\gamma = 0^\circ$). In the case of curve *d* also the locality and the freedom-of-choice loopholes were addressed.

Microwave Background frame ($\beta \approx 10^{-3}$, $\chi \approx 97^\circ$) we get $\beta_{t,\max} \approx 5 \times 10^6$. The other curves represent the experimental values of $\beta_{t,\max}$ obtained in the previous experiments [22, 23, 26].

In conclusion, no evidence for the occurrence of superluminal communications has been found in our experiment and a higher lower bound for the speed of the superluminal has been established. We remind here that, due to the inclination of our apparatus with respect to the east-west direction, we are not sensitive to about a 5% of all the possible orientations of the velocity vector of the preferred frame and that our experimental results have been obtained under the assumption that the collapse of the polarization state occurs at the absorption polarizers.

Acknowledgements

We acknowledge the Fondazione Pisa for financial support. We acknowledge the EGO and VIRGO staff that made possible the experiment and, in particular, F. Ferrini, F. Carbognani, A. Paoli and C. Fabozzi. We are especially grateful to M. Bianucci (Pisa Physics Department) and to S. Cortese (VIRGO) for their invaluable and continuous contribution to the solution of many electronic and informatic problems. Finally, we acknowledge N. Gisin for helpful comments and T. Faetti for helpful suggestions on real-time procedures.

References

- [1] Einstein A, Podolsky B and Rosen N 1935 *Phys. Rev.* **47**(10) 777–780
- [2] Bell J S 1964 *Physics* **1** 195–200
- [3] Clauser J F, Horne M A, AShimony and Holt R 1969 *Phys. Rev. Lett.* **23**(2) 880
- [4] Clauser J F and Horne M A 1974 *Phys. Rev. D* **10**(2) 526

- [5] Aspect A, Dalibard J and Roger G 1982 *Phys. Rev. Lett.* **49**(25) 1804–1807
- [6] Hensen B *et al.* 2015 *Nature* **526** 682
- [7] Giustina M *et al.* 2015 *Phys. Rev. Lett.* **115**(25) 250401
- [8] Shalm L K *et al.* 2015 *Phys. Rev. Lett.* **115**(25) 250402
- [9] Rosenfeld W, Burchardt D, Garthoff R, Redecker K, Ortegel N, Rau M and Weinfurter H 2017 *Phys. Rev. Lett.* **119**(1) 010402
- [10] Newton, letter to R Bentley, 1692/3,189R447, f 6, Trinity College Library, Cambridge, UK
- [11] Abbot B P *et al.* 2016 *Phys. Rev. Lett.* **116**(25) 061102
- [12] Davies P C W and Brown J R 1986 *The ghost in the atom: a discussion of the mysteries of quantum physics* canto ed. ed (Cambridge; New York: Cambridge University Press)
- [13] Coccia B 2013 *Physics Essays* **26** 531–547
- [14] Coccia B 2015 *Journal of Physics: Conference Series* **626** 012054
- [15] Eberhard P H 1989 A realistic model for quantum theory with a locality property *Quantum theory and pictures of reality: foundations, interpretations, and new aspects* ed Schommers W (Berlin; New York: Springer-Verlag) pp 169–2016
- [16] Bohm D and Hiley B J 1993 *The undivided universe: an ontological interpretation of quantum mechanics* (Routledge, London,)
- [17] Gisin N 2014 *Quantum Correlations in Newtonian Space and Time: Faster than Light Communication or Nonlocality* (Milano: Springer Milan) pp 185–203
- [18] Bancal J, Pironio S, Acín A, Liang Y, Scarani V and Gisin N 2012 *Nat. Phys.* **8** 867–870
- [19] Coccia B, Faetti S and Fronzoni L 2018 *Phys. Rev. A* **97**(5) 052124
- [20] Aspect A 2002 Bell's theorem: The naive view of an experimentalist *Quantum (Un)speakables: From Bell to Quantum Information* ed Bertlmann R A and Zeilinger A (Springer)
- [21] Coccia B, Faetti S and Fronzoni L 2017 *Journal of Physics: Conference Series* **880** 012036
- [22] Salart D, Baas A, Branciard C, Gisin N and Zbinden H 2008 *Nature* **454** 861–864
- [23] Coccia B, Faetti S and Fronzoni L 2011 *Phys. Lett. A* **375** 379–384
- [24] European Gravitational Observatory, <https://wwwego-gw.it/> URL <https://www.ego-gw.it>
- [25] Barnea T J, Bancal J D, Liang Y C and Gisin N 2013 *Phys. Rev. A* **88**(2) 022123
- [26] Yin J *et al.* 2013 *Phys. Rev. Lett.* **110**(26) 260407
- [27] Kwiat P G, Waks E, White A G, Appelbaum I and Eberhard P H 1999 *Phys. Rev. A* **60**(2) R773–R776
- [28] Altepeter J, Jeffrey E and Kwiat P 2005 *Opt. Express* **13** 8951–8959
- [29] Akselrod G M, Altepeter J B, Jeffrey E R and Kwiat P G 2007 *Opt. Express* **15** 5260–5261
- [30] Rangarajan R, Goggin M and Kwiat P 2009 *Opt. Express* **17** 18920–18933
- [31] PK Seidelmann B Guinot L D 1992 *Explanatory Supplement to the Astronomical Almanac, cp.2* (US Naval Observatory, University Science books, Mill Valley, CA)
- [32] National Radio Astronomy Observatory, Rick Fisher homepage, <https://www.cv.nrao.edu/~rfisher/Ephemerides/times.htm>
- [33] I R 2012 *A Dictionary of Astronomy, 2nd.ed* (Oxford: Oxford University Press)